コンクリート工学年次論文報告集, Vol.16, No.2, 1994

論 文

[2140] An Experimental Study on Joint Strength of Spliced Bars for Precast Concrete Structures with Double Layer Reinforcements

Rodolfo YANEZ*1, Akitoshi HATAHIRA*2, Teruaki YAMAGUCHI*3 and Hiroshi IMAI*4

1. INTRODUCTION

To study the effect of the proposed bar joint [1,2] on the joint strength of specimens with double layer reinforcement, another series of pullout tests was carried out. Many problems have to be solved to joint double layer main bars with lapping splices. One of the practical solutions is to joint the half of bars at the same section and to joint the other half of bars at different section. A number of combinations of bars (combinations among spliced bars and continuous bars) which are possible to use at the construction sites are selected. The joint strength of these combinations of jointed and continuous main bars are herein studied.

2. TEST SPECIMENS

Table 1 shows the differences among the test specimens. The specimens were designed to represent a confined section of precast concrete columns or beams. They were divided into six different cases. Each case has a different distribution of spliced bars and continuous bars in the first and second layers. Two specimens per each case were tested. Two specimens have a single layer of reinforcement. The specimens, with sections of 450-mm x 600-mm (single layer reinforcement) and 450-mm x750-mm (double layer reinforcement), have both horizontal and vertical distances of 100-mm between the bar axes. The section of typical specimens are shown in Fig. 1.

Bars D25 (SD490) and bars D25 (SD390) were chosen as main bars for the single and double layers, respectively. For lapping bars of specimens with double layers, eight specimens have two bars D19 (SD490), and two specimens have one bar D25 (SD490) per a main bar. The single layered specimens have also 2-D19 (SD490) lapping bars. Thus, the sectional area of the lapping bars are equal or greater than that of the main bars. Also, a supplementary reinforcement was placed to restrain the propagation of cracks to the other side of the specimen during loading.

The lapping length which is 15 times the lapping bar diameter, 15d, was used for all the double layer specimens. For the single layer a lapping length of 20d was used.

---

*1 Graduate School, University of Tsukuba, M.Sc., Member of JCI
*2 Undergraduate Student, University of Tsukuba, Member of JCI
*3 Technical Research Institute, Kabuki Construction Co. Ltd., Member of JCI
*4 Institute of Engineering Mechanics, University of Tsukuba, DR, Member of JCI

Table 1. Differences among specimens

	Spec No.	Section	Length (mm)	Main bars	Lateral reinforcement	Lapping bars	Lapped length	Position of bars	Layer
Single layer	PC 31	450 x 600	1000	D25 (SD490)			20d 380 mm	J-C -J-C	single layer
Double layer	PC 32							J -J -J -J J -J -J -J	1st 2nd
	PC 33				4-D10@100	2-D19 (SD490)		J -C-J-C C -J-C-J	1st 2nd
	PC 34	450 x 750	800	D25 (SD390)	(SD295A)		15d 285 mm	C-C-C-C J -J -J -J	1st 2nd
	PC 35							J -J -J -J C-C-C-C	1st 2nd
	PC 36		1000			1-D25 (SD490)	15d 375 mm	J-J'-J -J J-J -J -J	1st 2nd

Fc=300 kgf/cm ^{2}
C: continuous main bar
J: jointed main bar
d: diameter of lapping bar

Specified strength of mortar=600 kgf/cm ^{2}
Sheath diameter =42 mm
Cover thickness =40 mm

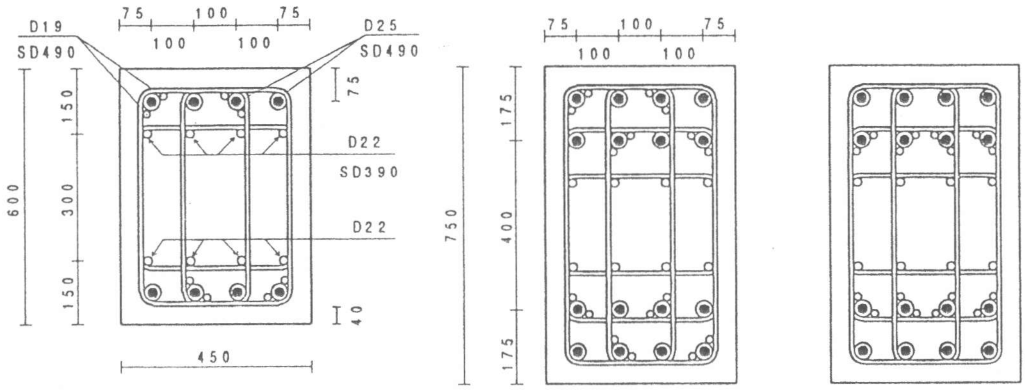

a) PC31 b) PC33 c) PC34

Fig. 1 Section of specimens

For all the specimens, continuous and jointed bars were inserted into the sheaths positioned vertically and high strength mortar was pre-grouted. The bar ends were abutted at the center of sheath. The concrete was cast horizontally.

The common parameters for all specimens were: a steel spiral sheath of 42 mm diameter with lug height of 2 mm and lug distance of 28 mm, cover concrete of 40 mm from the surface to the lateral reinforcement, and lateral reinforcement of 4-D10 (SD295A) @100-mm.

The specified compressive strengths of the concrete and the grout mortar were Fc= 300 kgf/cm^2 (29.4 MPa) and 600 kgf/cm^2 (58.8 MPa), respectively. Properties of concrete, grout mortar and steel are shown in Tables 2, 3 and 4, respectively. Each value is the average of three test pieces. The grout mortar pieces were tested a month after grouting.

Table 2. Properties of concrete

Specimen	Concrete Strength (kgf/cm ^{2})		
	Compressive		Tensile
	4 Weeks	Experimental day	
PC-31,32,33	303	327	24.5
PC-34,35,36	315	327	30.3

Fc: 300 kgf/cm ^{2}

Table 3. Properties of mortar

Mortar Strength (Kgf/cm ^{2})		
Days	Grouting	
	First	Second
7	558	492
28	628	623
81	663	647

Fc: 600 kgf/cm ^{2}

3. TEST APPARATUS AND LOADING HISTORY

The test setup is shown in Fig. 2. Tension force P was applied horizontally at both ends of each main bar by four oil jacks (each side) controlled by a load cell. In case of the double layer specimens, high strength bars D32 were used to transmit the pulling forces from the oil jacks to the specimen main bars. Each connection among two tested main bars 2-D25 and the high strength bars D32 was made using a thick steel plate and nuts.

Displacement between the ends of each main bar was also measured. Two sets of measuring devices were placed at the corner and side bars. The displacement δ at the axis of each bar (corner or side) was obtained by extrapolating the measurements of δ_a and δ_b. Strain gauges were placed at the bars of the 1st and 2nd layers outside of the specimen length to trace the distribution of load. No differences among the pulling forces of the first and second layers were observed from the readings of the strains in the main bars.

Table 4. Properties of steel

Bar	Grade	Yield Stress σ_y (kgf/mm^2)	Tensile Stress σ_B (kgf/mm^2)	Young's Modulus x10^3 (tf/cm^2)
D25	SD390	43.6	63.0	1974
D25	SD490	50.7	69.4	1938
D19	SD490	50.9	69.1	1972
D10	SD295A	37.0	51.2	1996

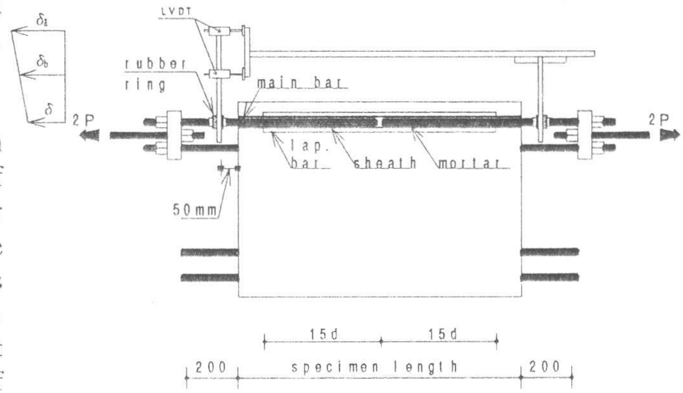

d: diameter of lapping bars

Fig. 2 Loading apparatus

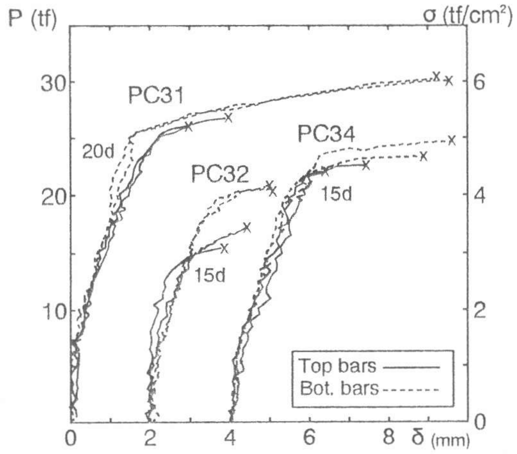

Fig. 3 Typical P-δ of PC31, PC32 and PC34

4. FAILURE PATTERN AND LOAD-DISPLACEMENT RELATIONSHIPS

The main bar, grouted mortar, and sheath behaved as a single unit, because the main bars were not pulled out of the sheaths.

Load-displacement relations for each specimen are presented in Fig. 3. The specimen with a single layer reinforcement (PC31) shows almost the same maximum load for the top and bottom bars. Also, these values were higher than the maximum loads of the specimens with double layer reinforcement.

For PC32 with bars jointed at the first and second layer, the maximum load of the bottom bars were 1.3 times greater than that of the top bars. Until 10 tf, the specimen has a curve similar to PC31, and for load greater than 10 tf a decay on the stiffness is observed.

PC34 with double layer reinforcement with a distribution of continuous bars in the first layer and jointed bars in the second layer shows almost the same maximum loads for the top and bottom bars.

The typical crack patterns for specimen PC31 with a single layer of reinforcement and for PC34 with double layer reinforcement are shown in Figs. 4(a) and (b). In all specimens, first transverse cracks appeared at 1/3 the specimen length at an average load of 5 tf. As the load increases transverse cracks developed at the center and along the direction of bars at both ends. Cracks spread with the increment of load. Before reaching the maximum load a concentration of inclined cracks at both sides of the specimen was observed. A side splitting failure pattern was noticed in all specimens.

PC31 showed that there were fewer longitudinal cracks for the bottom bars than for the top bars. In the bottom bars, before the maximum load is attained, the transverse crack developed at the center, then spread from side to side and the specimen failed at the center. The top bars failed at the corner of the specimen where bars with lapping splices are positioned.

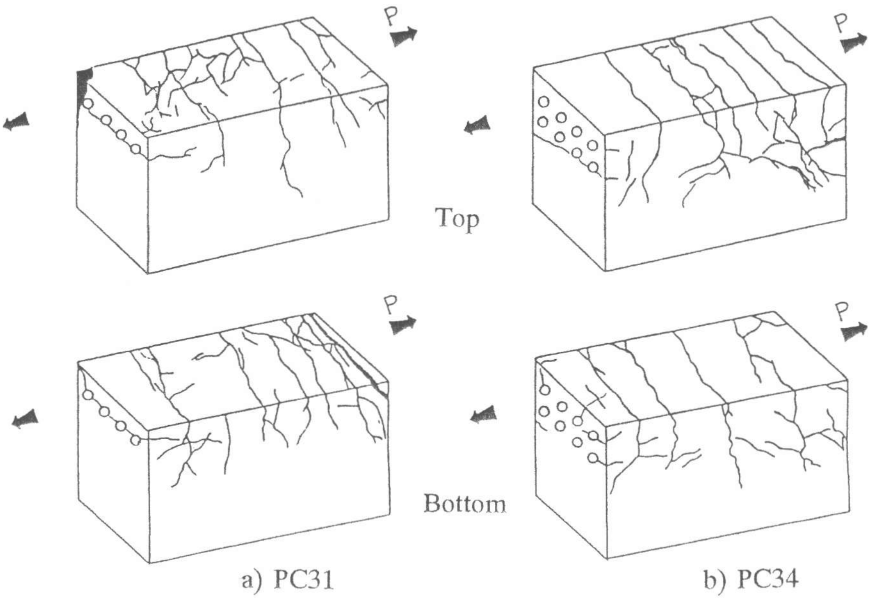

Fig. 4 Typical crack pattern of PC31 and PC34

In case of PC34, having the distribution of continuous bars in the first layer and jointed bars in the second layers, crack pattern is similar to that of PC31, but with a less number of longitudinal cracks. Transverse cracks appeared at 1/5 the specimen length. Before the maximum load longitudinal cracks appeared at both ends of the specimen. For the top bars, at the pulling face the failure line started from the position of bars with lapping splices in the second layer and spread from side to side. Because of the additional reinforcement, no effect of the previous test (i.e. for the same specimen, testing the bottom bars after the test of the top bars), on the crack pattern was recognized.

5. TEST RESULTS

5.1 Relationship among the top and bottom bars

The relationship between the maximum strengths of the top and bottom bars is shown in Fig. 5. The maximum loads of the bottom bars were on the average 1.15 times greater than those of top bars. This value differs from the values obtained in the joint strength test of lapping splices [1,2], where it was 1.37.

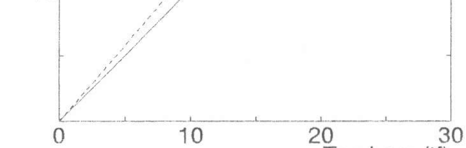

Fig. 5 Relationship among top and bottom bars

5.2 Comparison with the existing equations

The experimental bond strength (τ_{exp}) was deduced by converting the applied maximum forces acting in one bar into bond stresses using Eq. (1). Also, bond splitting strengths are calculated using the formulas proposed by Fujii–Morita [3] Eq. (2), τ_{cm}, Orangun–Jirsa–Breen [4] Eq. (3), τ_{coj} and Kaku–Zhang–Iizuka–Yamada [5] Eq. (4 (a) and (b)), τ_{ck}.

$$\tau_{exp} = \frac{Pmax}{ls\phi} \qquad (1)$$

$$\tau_{cm} = (0.307 b_i + 0.427 + 24.9 \frac{kA_{st}}{sN_t d_b}) \sqrt{\sigma_B} \cdots\cdots\cdots\cdots \quad (2)$$

$$\tau_{coj} = (1.2 + 3\frac{c}{d_b} + 50\frac{d_b}{ls} + \frac{A_w {}_w\sigma_y}{35.2 N_t s d_b}) 0.265 \sqrt{\sigma_B} \cdots\cdots \quad (3)$$

$$\tau_{ck} = [0.08 + 0.12 b_i + k_n (\frac{2.5 + 875 p_w}{l_b/d_b + 7000 p_w} + 18.0 \frac{p_w\, b}{N d_b})] \sigma_B^{0.6} \qquad (4a)$$

if $\sigma_{wy} \leq 115\sigma_B^{0.6}$:

$$\tau_{ck} = [0.08 + 0.12 b_i + k_n (\frac{2.5 + 875 p_w}{l_b/d_b + 7000 p_w} + 18.0 \frac{p_w\, b}{N d_b})] \frac{\sigma_{wy}}{115} \qquad (4b)$$

$$k_n = 1 + 0.85 \frac{(n-2)}{N}$$

Where:

Pmax: maximum force in the main bar (kgf);

ϕ : perimeter of bar or sheath (cm);

$l_b = l_s$: lapped length (cm);

b_i: parameter of the clear distance of main bars;

k: parameter of failure pattern;

$A_{st} = A_w$: area of lateral reinforcement (cm^2);

N_t: total number of main bars;

n: number of tie legs;

d_b: diameter of sheath (cm);

b: width of beam (cm);

$f_{yt} = {}_w\sigma_y$: yielding strength of lateral reinforcement (kgf/cm^2);

c: half clear spacing of bars in the failure plane (cm);

s: spacing of the lateral reinforcing bars (cm);

σ_B: concrete cylinder strength (kgf/cm^2);

$p_w = \rho_v$: lateral reinforcement ratio.

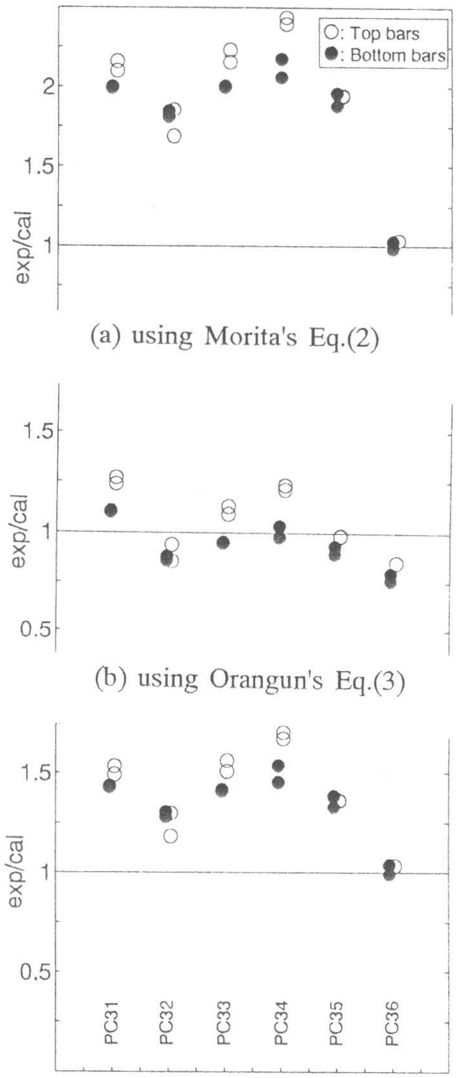

(a) using Morita's Eq.(2)

(b) using Orangun's Eq.(3)

(c) using Kaku's Eq.(4)

Fig. 6 Comparison with existing equations

The ratio of the experimental bond strength τ_{exp} and the calculated bond strengths (τ_{cm}, τ_{coj}, τ_{ck}) are compared in Fig. 6. The side splitting failure patterns proposed in [2] are used based on the observed failure modes.

It is observed in Fig. 6(a) that the ratios in PC36 (with one lapping bar D25) are equal to 1, while the others are almost 2 with a large scatter. Orangun's equation (τ_{coj}) has a good agreement with the test results, as it is shown in Fig. 6 (b).

In Fig. 6 (c), the Kaku's equation shows a good agreement for the PC36 with one lapping bar, while the others are at the level of 1.5, same as for the Fujii–Morita equation.

5.3 Comparison of the strength of double layer reinforcement with that of a single layer reinforcement

The test results of specimens with double layers are also compared with those of the specimens with a single layer reinforcement in terms of the average bond strength per unit surface are as it is shown in Fig. 7.

No great difference on the joint strength for the specimens with a single layer reinforcement of jointed bars and specimens with double layer reinforcement is recognized. However, PC31 with an arrangement of continuous and jointed bars among a single layer showed in terms of maximum load a higher joint strength than the specimens with double layer reinforcement.

5.4 Effect on the joint strength of the combinations of bars

The effect on the joint strength of the combinations of bars is shown in Fig. 7. The better combination of bars is that made of continuous bars in the first layer and jointed bars in the second layer. For this combination, no great difference of the test results from the top and bottom bars is recognized.

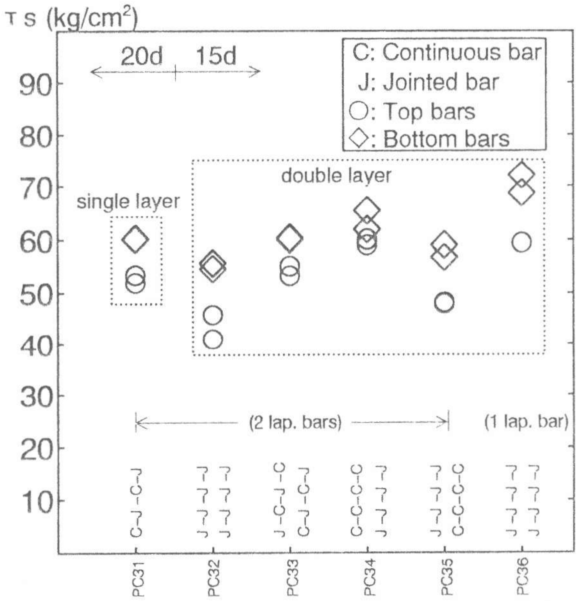

Fig. 7 Effect on the joint strength of the combinations of bars

6. CONCLUSIONS

The results of the present chapter are summarized as follows:

1) No great difference on the joint strength for the specimens with a single layer reinforcement of jointed bars and specimens with double layer reinforcement is recognized.
2) The maximum load acting per bar among the double layer reinforcement can be considered for the calculation of the bond strength.
3) No remarkable difference on the joint strengths of the bars placed at the first and second layers is recognized.
4) The Orangun–Jirsa–Breen's equation gives a good accuracy for the estimation of the bond strength of bars with lapping splices.

REFERENCES

1. Yanez, R. et al., "An Experimental Study on the Strength of a Proposed Bar Joint for Precast Concrete Columns", Proceedings of JCI, Vol. 14, No. 2, 1992, pp. 999–1004.
2. Yanez, R. et al., "An Experimental Study on Joint Strength of Spliced for Precast Concrete Structures", Transactions of The Japan Concrete Institute, Vol. 15, 1993, pp. 565–572.
3. Fujii, S.; Morita, S., "Splitting Bond Capacity of Deformed Bars (Part 2), (in Japanese)", Transactions of AIJ, No. 324, Feb. 1983, pp. 45–53.
4. Orangun, C.O.; Jirsa, J.O.; Breen, J.E., "A Reevaluation of Test Data on Development Length and Splices", ACI Journal, Vol. 74, March, 1977, pp. 114–122.
5. Kaku, T. et al., "A Proposal of Equation for Bond Splitting Strength of Reinforced Concrete Members Including High Strength Concrete Level (in Japanese)", Concrete Research and Technology, Vol. 3, No. 1, Jan. 1992, pp. 97–108.